



# Unexpected obstacles in mechanical recycling of polypropylene labels: Are ambitious recycling targets achievable?

Jessica Schlossnikl<sup>a,\*</sup>, Elisabeth Pinter<sup>b</sup>, Mitchell P. Jones<sup>a</sup>, Thomas Koch<sup>a</sup>, Vasiliki-Maria Archodoulaki<sup>a,\*</sup>

<sup>a</sup> Institute of Materials Science and Technology, Faculty of Mechanical and Industrial Engineering, TU Wien, Gumpendorferstrasse 7, Object 8, 1060 Vienna, Austria

<sup>b</sup> OFI Austrian Research Institute for Chemistry and Technology, Department for Packaging, Recycling and Dangerous Goods, Franz-Grill-Strasse 5, Object 213, 1030 Vienna, Austria

## ARTICLE INFO

**Keywords:**  
Labels  
Polypropylene  
Recyclability  
Toxicology  
Circular economy

## ABSTRACT

Recycling initiatives like the ‘Green Deal’, aspire to achieve complete recyclability for packaging materials and previously overlooked recycling fractions, but they might face practical challenges. We investigated the mechanical, processing, and toxicological properties of polypropylene labels during mechanical recycling to gain insight into dealing with as yet unutilized recycling fractions. Possible challenges during recycling include label pigments shifting infrared spectra bands and promoting  $\beta$ -spherulite nucleation, which can cause homopolymer melting peaks to resemble copolymers or multilayered structures. Label blends also do not conform to the straightforward rules of linear mixing. This means that predicting mold and machine parameters for blends of virgin and recycled material becomes challenging. The elongation at break of these blends is also influenced by the presence of labels, with noticeable deterioration effects even at label concentrations as low as 20 wt.%. Moreover, labels contain substances classified as Cramer Class III, with DNA-reactive mutagenicity responses present in processed and unprocessed labels. Despite labels ultimately being recyclable and potentially repurposable for extrusion or injection molding applications, their complex processing requirements, safety concerns, and limited economic viability may make them more valuable indirectly, on a systemic level, providing useful information for consumers including on the disposal and recyclability of packaging.

## 1. Introduction

Recycling would appear to be everywhere, and its alternatives are increasingly less socially acceptable (Clapp, 2012) and yet only 35% of European plastic consumer waste was recycled in 2020. Most plastic waste in Europe is thermally recovered (42%) but a considerable portion (23%) still ends up in landfill (Plastics Europe, 2022). These realities in addition to scientific consensus on the effects of climate change and shifting social norms are driving more ambitious recycling legislation included in the Green Deal, which comprises a series of policies and regulations aimed at promoting circular economy in the EU. Among these recent reforms, the Packaging and Packaging Waste Directive (PPWD) was revised to stipulate that all packaging must be either reusable or recyclable in an economically viable manner by 2030, with a target of 100% recyclability in all packaging (ECR Austria, 2022; European Commission, 2022).

The future of recycling will include many previously unconsidered

and as yet academically and industrially neglected recycling fractions including labels. Labels traditionally serve an informative and esthetic function for products, providing consumers with information on ingredients, nutrition, and allergens, (White, 2012; Marchini *et al.*, 2021), in addition to serving an inventory and logistics function for supermarkets and supply chains and providing marketing space for branding (Rundh, 2005; Klimchuk and Krasovec, 2012). They have, however, never been considered an economically viable fraction for mechanical recycling due to their low quantities (~65,160 tons/year in the EU27 + UK based on a label that comprises  $1.81 \pm 0.48\%$  (Table S2) of the total packaging mass and a PET bottle market volume of 3.6 MT in 2020 (EUNOMIA, 2022)) and potential processing hazards originating from inks, pigments, and other additives (FH Campus Wien, 2020).

Bottles are typically shredded without prior removal of caps or labels, the labels wind sifted, rejected, and incinerated. Shredded bottles and caps are then separated using a swim-sink process into a polyethylene terephthalate (PET) fraction and a mixed polypropylene (PP)

\* Corresponding author.

E-mail addresses: [jessica.schlossnikl@tuwien.ac.at](mailto:jessica.schlossnikl@tuwien.ac.at) (J. Schlossnikl), [vasiliki-maria.archodoulaki@tuwien.ac.at](mailto:vasiliki-maria.archodoulaki@tuwien.ac.at) (V.-M. Archodoulaki).

and polyethylene (PE) fraction (Neubauer et al., 2021). Polymer contamination (PP in PE or vice versa) can result in different deformation mechanisms in recycled blends, which have important ramifications for recycling (Van Belle et al., 2020; Karaagac et al., 2021). Clean flexible material, such as labels, can be mechanically recycled (Horodytska et al., 2018) but coloring and printing impurities in labels can lead to reduced mechanical properties and luminous transmittance levels (Gabriel and Maulana, 2018). The presence of up to 1 wt.% virtually unremovable PP label contamination in waste electrical and electronic equipment (WEEE) can also cause small changes in the mechanical properties of acrylonitrile butadiene styrene (ABS) and polyvinyl chloride (PVC) (Kühnel et al., 2019). Scope of application for recycled labels has otherwise been limited to use as a foaming agent (21% labels) (Guillén-Mallete et al., 2021).

Alternatives to labels, such as shrink sleeves can also be used to protect bottles. Both labels and sleeves may play a systemic role enabling recyclability of base packaging material by isolating higher concentrations of pigments and other printing additives to a single easily removed packaging component (Gabriel and Maulana, 2018). Sleeves have the advantage of not requiring adhesives but are hard to detect using near infrared (NIR) sorting, especially if they contain a large, printed surface area. Sleeves are commonly produced from PET, polystyrene (PS) and PVC, materials which may not match the bottle material, resulting in misidentification of the packaging during sorting (Chen et al., 2022). Labels are typically favored over sleeves due to their smaller size, which is not only more efficient in terms of material use but also facilitates easier and more accurate sorting (Cotrep, 2022). To date, the recyclability of labels represents a scarcity in the literature but will likely become more relevant to the future of recycling.

We conducted a comprehensive investigation into the mechanical recyclability of PP labels to provide foundational information on their recycling characteristics but more importantly to demonstrate the unique range of unanticipated considerations that one must confront when working with as-of-yet poorly characterized recycling fractions. The mechanical and processing properties of pre- and post-consumer PP labels and virgin-recyclate blends were characterized and noteworthy morphological features and toxicology data collected.

## 2. Materials & methods

### 2.1. Materials

PET bottles were collected from post-consumer recycling bins in eastern Austria and their labels removed. Pre-consumer labels were kindly provided by AluPrint (Vrútky, Slovakia) to enable comparison between pre- and post-consumer labels. PPHD601CF PP was kindly provided by Borealis (Vienna, Austria) to serve as a virgin reference for the base material of the pure labels and to investigate virgin-recyclate blends. This PP was selected due to its similar melt mass-flow rate (MFR) to the label material and similar intended application. Post-consumer material was hand-washed with a mixture of water and detergent upon collection and rinsed with tap water. Labels were identified based on a combination of visual and haptic properties coupled with attenuated total reflection (ATR) Fourier transform infrared (FT-IR) spectroscopy. PP labels were retained while others were discarded. This screening process simplified the label stream and consequently reduced the likelihood of complex deformation phenomena associated with polymer contamination (Van Belle et al., 2020). In principle, industrial solutions exist for the separation of PP and PE (Bakker et al., 2009; Serranti et al., 2015). However, due to cost and efficiency restrictions, current industrial practice would likely see this stream end up in a mixed polyolefin fraction (Cotrep, 2022; Grüner Punkt, 2023). All other material was used as received.

### 2.2. Thermal and morphological analysis of the labels

Differential scanning calorimetry (DSC) is used to sample recycling batches for polymer impurities (Achilias, 2022), however, only rough approximations of impurity concentration can be achieved using this method (Juan et al., 2021; Thoden van Velzen et al., 2021). Pre-consumer labels were analyzed both before and after processing (extrusion) using a TA Instruments Q 2000 DSC (TA Instruments, New Castle, DE, USA). A  $5 \pm 0.5$  mg sample mass of each label or polymer granule was deposited in an alumina testing pan and sealed. Samples were heated from 20 to 200 °C at 10 K/min, cooled at the same rate to 20 °C, and then reheated under the same heating conditions as previously described. A nitrogen atmosphere was maintained at all times using a flow rate of 50 mL/min. The melting temperature  $T_m$  of the second heating run was analyzed using TA Instruments Software TRIOS 5.1.1. Analysis was based on three replicate specimens for each sample type.

The penetration depths of NIR and ATR FT-IR technologies are dependent on the absorbance of the sample material at the respective wavelengths. NIR tends to be less sensitive to surface features and is commonly used in sorting polymer-based household waste (Eisenreich and Rohe, 2006; da Silva and Wiebeck, 2020; Cozzarini et al., 2023). ATR FT-IR is more suitable for assessing pigments, additives, and other surface characteristics. Examples of additives that can be detected by FT-IR include the optical brightener Uvitex (Mauricio-Iglesias et al., 2009) and antioxidants Irganox 1010 and 1076 (Saunier et al., 2017; Zheng et al., 2020; Zheng and Fan, 2022). IR spectra were recorded using a Bruker TENSOR 27 FT-IR instrument (Bruker, Billerica, MA, USA) with an ATR diamond (DuraSample IR II) with single reflection. Three sites were measured across three replicate labels for all label types. 16 scans were conducted in the mid-IR spectrum between 600 and 4000  $\text{cm}^{-1}$  with a resolution of 4  $\text{cm}^{-1}$ , which contains the fingerprint region where polymers can be detected more specifically (Siesler et al., 2002; Nandiyanto et al., 2019).

To observe spherulitic morphology, injection molded tensile impact strength specimens prepared from pre-consumer labels were sliced through their cross section (thickness of 30  $\mu\text{m}$ ) using a Microm HM 360 Microtome (Microm, Germany). Specimens were heated and cooled using a temperature program matching that adopted for DSC measurements utilizing a THMS 600 Linkam microscope temperature stage (Linkam scientific instruments, UK), and imaged using a Zeiss Axio Lab (Carl Zeiss Microscopy, Germany) optical microscope. Pre-consumer labels with a thickness of 35  $\mu\text{m}$  were investigated as received in the same way. Mixing quality was evaluated using gold sputtered fracture surfaces of tensile impact tested specimens and a Zeiss EVO 10 (Carl Zeiss Microscopy, Germany) scanning electron microscope (SEM) at an accelerating voltage of 3 kV.

### 2.3. Extrusion of label-virgin blends

Pre- and post-consumer labels were mixed in increments of 10 wt.% from 10–50 wt.% with virgin PP. Pure pre- and post-consumer labels and label-virgin blends, were extruded using a single screw extruder (EX-18–26–1.5, Extron Engineering Oy, Finland) with a screw diameter of 18 mm, length-to-diameter ratio of 25:1 at 240 °C and 70 rpm screw speed. The extruded material was then ground into flakes using a mill (Fritsch Pulverisette 19, FRITTSCH GmbH, Germany), and a sieved fraction of 4 mm was collected.

The linear mixing rule (Eq. (1)) was utilized during blending as the use of logarithmic or natural logarithmic mixing rules yielded negligible difference in calculated zero-shear viscosity  $\eta_0$ . The linear mixing rule also serves as a good approximation for blends with minimal MFR differences (Traxler et al., 2023).  $\eta_0$  was calculated using the linear mixing rule by summing the respective weight fraction ( $x_i$ ) multiplied by the respective viscosity ( $\eta_i$ ) of the components.

$$\eta_0 = \sum_i x_i \eta_i \quad (1)$$

#### 2.4. Injection and compression molding of label-virgin blends and preparation of the mechanical and rheological test specimens

Pure pre- and post-consumer labels and label-virgin blends were injection molded to prepare tensile (impact) strength specimens using a Haake Mini Lab II twin screw extruder coupled with a Haake Mini Jet II injection molding unit (Thermo Fisher Scientific, Waltham, MA, USA). Extrusion was completed at 230 °C with a screw speed of 100 rpm. Injection molding was completed at a mold temperature of 40 °C and a pressure of 350 bar with injection and post-injection times both of 10 s. At least eight dog-bone tensile (thickness  $2 \pm 0.2$  mm) and tensile impact test specimens (thickness  $1.2 \pm 0.06$  mm) were molded in accordance with ISO 527-2-5A (The International Organization for Standardization, 2012b) and ISO 8256/1A (The International Organization for Standardization, 2004), respectively. Tensile impact test specimens were notched on both sides (each 2 mm) with a Notch-Vis tool (Ceast, Germany).

Pure pre- and post-consumer labels and label-virgin blends were compression molded (Collin P 200 P, Germany) using an aluminum pattern sandwiched between Teflon® and steel plates at 210 °C and 50 bar with a cooling rate of 15 K/min to prepare dynamic shear rheology test specimens for all materials in accordance with ISO 19,069-2:2016 (The International Organization for Standardization, 2020). Disk-shaped specimens were produced with a diameter of 25 mm and a height of 1.2 mm.

#### 2.5. Tensile (impact) testing and rheological testing of label-virgin samples

A universal testing system comprising a Zwick 050 frame, 2.5 kN load cell and extensometer (Zwick Roell, Germany) was used to perform tensile tests on the prepared specimens at a constant velocity of 20 mm/min. The elastic modulus  $E_r$ , yield stress  $\sigma_y$ , and elongation at break  $\varepsilon_B$  were calculated using the ZwickRoell testXpert II software (v. 3.6) across six replicate tests. An Instron 9050 impact pendulum (Ceast, Pianezza, Italy) equipped with a 2 J hammer and 15 g crosshead mass was used to establish the tensile impact strength  $a_{IV}$  of the notched samples across at least eight replicates.

Dynamic shear rheology was tested using frequency sweeps on a MCR 302 rheometer (Anton Paar, Graz, Austria) equipped with a plate-plate system (1 mm gap size) and a heating hood purged with nitrogen. The temperature was constant at 230 °C during the experiments while deformation was raised logarithmically from 1% to 2% at a frequency ranging from 628 rad/s to 0.01 rad/s.  $\eta_0$  was selected at a frequency of 0.1 rad/s.

The MFR was measured for at least eight replicates of each sample according to ISO 1133-1 (The International Organization for Standardization, 2012a) at 230 °C under a 2.16 kg load on the MeltFloW basic (Karg Industrietechnik, Germany).

While  $\eta_0$  is correlated with material properties, such as molecular weight and branching structures (Dealy John et al., 2017), the MFR is used in quality management to assess the flowability of polymers at a given shear rate (Schroder, 2018).  $\eta_0$ , in principle, provided insight into how accurate and useful the MFR measurements were.

#### 2.6. Chemical and biological analysis of labels

Pure pre-consumer (before and after processing) and pure post-consumer (after processing only) labels were measured using gas chromatography-mass spectrometry (GC-MS) and *in vitro* bioassays (miniaturized Ames test). 5 g (for chemical analysis) and 30 g (for *in vitro* bioassays) samples, respectively, were immersed in 100 mL of ethanol (95%) and migrated at 60 °C for 10 days.

For GC-MS, 100  $\mu$ L ethanol migrate, 5 mL ultrapure water and 10  $\mu$ L internal standard (dodecan-d26) were applied. A pre-conditioned solid phase micro-extraction (SPME) sampler comprising 2 cm, 50/30  $\mu$ m divinylbenzene/carboxen/polydimethylsiloxane (DVB/CAR/PDMS) (Stableflex fibre, Supelco) was used to extract the samples at 80 °C for 20 min. Separation and identification was performed using an Agilent 6890 gas chromatograph with mass-selection detector HP 5975 (Agilent, USA), a quartz capillary (HP 5MS) and helium as a carrier gas. Substance identification was performed through comparison with a database (Wiley, National Institute of Standards and Technology) with acceptance criteria of >90 % match probability. Peak area was calculated but is not directly proportional to the concentration of the substances in the sample. Results can consequently only be considered qualitatively.

Identified substances were assessed using the ToxTree *in silico* decision tree tool and grouped into Cramer Classes I-III based on structural properties. Cramer Class II and III substances were considered more hazardous than Class I based on the structural alert for possible toxicity (Munro et al., 1996). Since only semi-quantitative concentration of the substances was possible and no oral consumption of the substances is expected, the application of safety thresholds based on Cramer Classes is not directly applicable. Nevertheless, these classes can provide insight into the level of toxicity of each substance.

For *in vitro* bioassays, samples were concentrated to 1 mL according to the protocol by Rainer et al. (2019) using a Syncore® Analyst device (Büchi, Germany) with a concentration factor of ~300. Dimethyl sulphoxide (DMSO) was added, and the remaining ethanol removed through evaporation until only the sample extract remained in DMSO. DMSO samples were applied to the miniaturized liquid Ames microplate format test with TA98 and TA100 strains as described by XENOMETRIX (2018) and Meyer et al. (2023). S9 experiments were completed using phenobarbital/ $\beta$ -naphthoflavone induced S9 provided by Xenometrix (Switzerland). Spiking experiments were also performed to assess interference effects from inhibiting/bacteriotoxic substances. All experiments were performed in triplicate with solvent blanks prepared and treated analogously.

### 3. Results and discussion

#### 3.1. Sorting- and quality management related label characterization

Transparent or uncolored labels exhibited IR bands at 972  $\text{cm}^{-1}$ , 1167  $\text{cm}^{-1}$ , 1375  $\text{cm}^{-1}$ , 1454  $\text{cm}^{-1}$ , 2839  $\text{cm}^{-1}$ , 2916  $\text{cm}^{-1}$  and 2949  $\text{cm}^{-1}$ , which are characteristic of PP (Jung et al., 2018). The presence of color coatings resulted in changes in the FT-IR spectra of labels, such as reductions in band intensity, omission, or addition of bands (Fig. 1). Most notable differences in the spectra of transparent, gray, red, and blue/orange colored PP labels were witnessed in the region 600–1800  $\text{cm}^{-1}$ , where the characteristic PP bands 972  $\text{cm}^{-1}$ , 1167  $\text{cm}^{-1}$ , 1375  $\text{cm}^{-1}$  and 1454  $\text{cm}^{-1}$  were often indistinguishable from other signals.

Printed parts of the labels exhibited an additional notable band between 1720–1728  $\text{cm}^{-1}$ , which may be attributable to C=O groups associated with organic pigments or additives, such as azo pigments (Ciccola et al., 2017) or adhesives (Chercoles Asensio et al., 2009). Blue/orange printed labels exhibited additional notable bands at 843  $\text{cm}^{-1}$  and 1643  $\text{cm}^{-1}$  (C–O stretching) (Singh Chouhan et al., 2020) most likely attributable to CaCO<sub>3</sub>, which is commonly used as a pigment in paints (Sun et al., 2018; Ersoy et al., 2021). That said, the many different components combined in paint, which exhibit their own characteristic bands, make any decisive identification of the combination of pigments present challenging (Tom Learner, 2004). Additional bands included 1067  $\text{cm}^{-1}$  (C–O–H) (Agbaje et al., 2017) and 1279  $\text{cm}^{-1}$  (C–H stretching) (Sepperumal and Markandan, 2014).

DSC curves exhibited a melting peak at 145–148 °C (Fig. 2). This peak was highly sensitive to processing, appearing very subtly in unprocessed samples but becoming very prominent after a single extrusion (processing). It should be noted that the location of this peak is quite

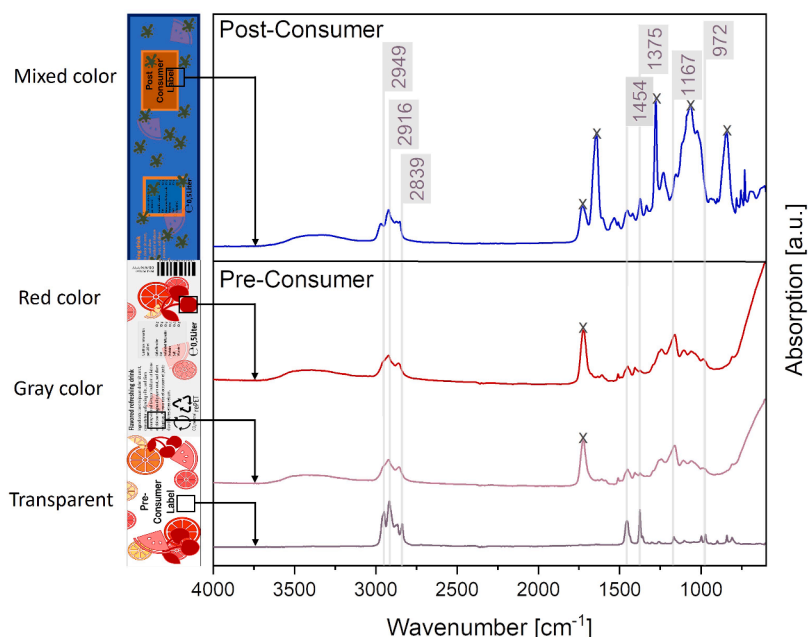


**Fig. 1.** Fourier transform infrared (FT-IR) spectroscopy of transparent, gray, red, and mixed color sections of pre- and post-consumer polypropylene (PP) labels. Notable bands (marked with crosses) at  $843\text{ cm}^{-1}$ ,  $1067\text{ cm}^{-1}$ ,  $1279\text{ cm}^{-1}$ ,  $1643\text{ cm}^{-1}$  and  $1720\text{--}1728\text{ cm}^{-1}$  differed from characteristic PP bands and were likely attributable to pigments or coatings in printed sections. (For interpretation of the references to color in this figure legend, the reader is referred to the web version of this article.)

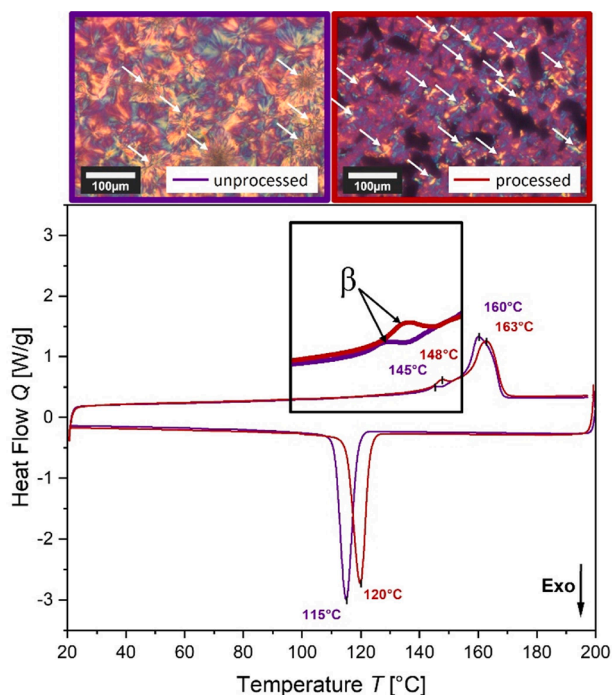


**Fig. 2.** Differential scanning calorimetry (DSC) thermograms of unprocessed (purple,  $T_m=145\text{ °C}$ ) and processed (red,  $T_m = 148\text{ °C}$ ) pre-consumer labels. These peaks are associated with  $\beta$ -spherulites (marked with arrows), shown in the corresponding micrographs. (For interpretation of the references to color in this figure legend, the reader is referred to the web version of this article.)

unfortunate since PP copolymers exhibit melting temperatures of  $135\text{--}150\text{ °C}$  (Gahleitner and Paulik, 2014) and this peak could subsequently be misinterpreted as being associated with a PP copolymer or multilayer structure during recycling quality management processes, which often incorporate DSC analysis (Grellmann and Seidler, 2011;

Achilias, 2022; Cozzarini et al., 2023). Further investigation using light microscopy revealed that the peak was, in fact, attributable to  $\beta$ -spherulites. Spherulite size was considerably smaller in processed labels, and black spots were visible in the micrographs. Color fragments (black spots in micrographs), such as pigments, can act as nucleating agents for  $\beta$ -spherulites (Tavanai et al., 2005) that are spread throughout the melt due to processing, causing nucleation to accelerate and resulting in smaller spherulites. Color fragments could be observed in SEM micrographs but did not form agglomerates (Figure S1). Polymer phase separation was also not visible.

### 3.2. Pre- and post-consumer label viscosity and processing parameters

Melt viscosity and processing parameters, measured as the industry standard MFR and  $\eta_0$  as an analytical reference, were unpredictable for both pre- and post-consumer labels in addition to blends thereof (Fig. 3). Notably, blends of both pre- and post-consumer labels and virgin material, that would typically be used to compensate for the poorer mechanical and processing properties of the recycled labels, did not follow linear mixing rules. The unpredictability of these blends means that recyclers may not be able to accurately predict the processing properties of their materials and may be forced to test and modify mold and machine parameters on a batch-by-batch basis at considerable effort and cost.

Increasing pre-consumer label material content in blends comprising labels and virgin PP resulted in variations in MFR (Fig. 3a). Variations in MFR could be attributable to complex chain scission events or the presence, lack or varying concentration of stabilizers (Saikrishnan et al., 2020; von Vacano et al., 2023). An unpredictable MFR or lack of consistency with the linear mixing rule are highly relevant to industry, which relies on the MFR to estimate flow properties to subsequently select processing parameters.

$\eta_0$  of blends comprising labels and virgin PP increased with increasing label content and exhibited a closer fit to the linear mixing rule (Fig. 3b). However, some samples did vary considerably from their expected values, in an indirectly proportional relationship with the MFR—a high MFR resulted in low viscosity and *vice versa* (Baur et al.,

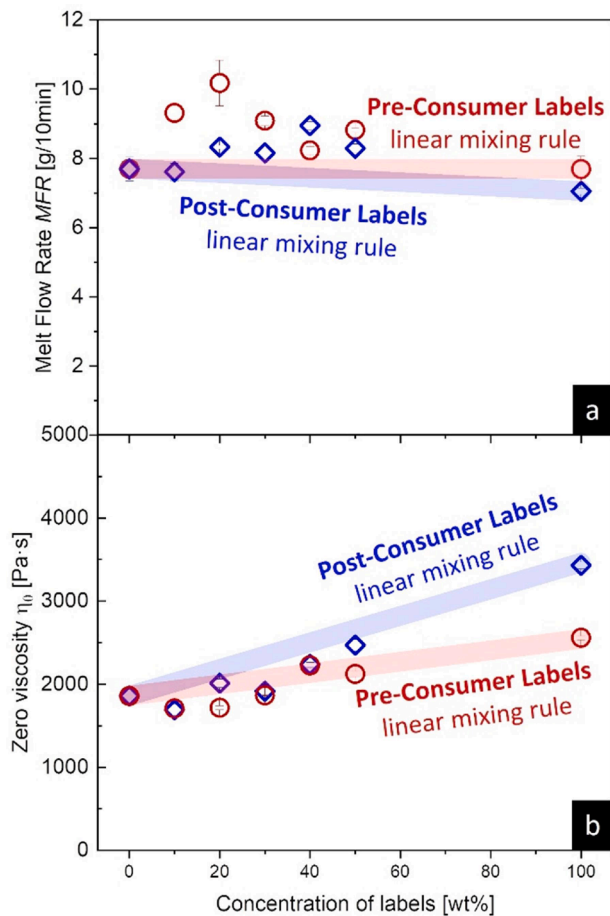


**Fig. 3.** (a) Melt flow rate (MFR, g/10 min) and (b) zero-shear viscosity ( $\eta_0$ , Pa·s) of pre- (red circles) and post-consumer (blue diamonds) labels. Calculated linear mixing rule is depicted using red and blue lines. (For interpretation of the references to color in this figure legend, the reader is referred to the web version of this article.)

2019). In fact, measured MFR typically fell above the value estimated using the linear mixing rule, while  $\eta_0$  fell below the linear mixing rule in most cases. Factoring in indirect proportionality,  $\eta_0$  data typically agreed with MFR data and validated the use of MFR for quality management. This is significant since  $\eta_0$  data is not available to most recyclers and consequently likely could not be used to inform recycling decisions.

### 3.3. Mechanical properties of blends of pre- and post-consumer labels and virgin PP

Pre- and post-consumer labels had a lower  $E_t$  (1351 MPa and 1431 MPa compared to 1777 MPa),  $\sigma_y$  (33.5 MPa and 32.0 MPa compared to 39.4 MPa), considerably lower  $\epsilon_B$  (476% and 512% compared to 839%) and approximately the same  $a_{IV}$  (38.5 kJ/m<sup>2</sup> and 41.7 kJ/m<sup>2</sup> compared to 40.6 kJ/m<sup>2</sup>) as virgin PP (Fig. 4). While not mechanically equivalent to virgin material, these properties indicated that recycled labels would still be mechanically suitable for extrusion or injection molding applications of PP with minimal esthetic and olfactory requirements, such as plant pots, storage boxes or waste containers (Christiani and Beckamp, 2020).

$\sigma_y$  decreased only slightly with the addition of either pre- or post-consumer labels to virgin PP, with an overall average reduction of 17% from pure virgin material to pure labels (Fig. 4a).  $E_t$  decreased incrementally with increasing pre-consumer label content with an overall decrease of 24% between pure pre-consumer labels to pure

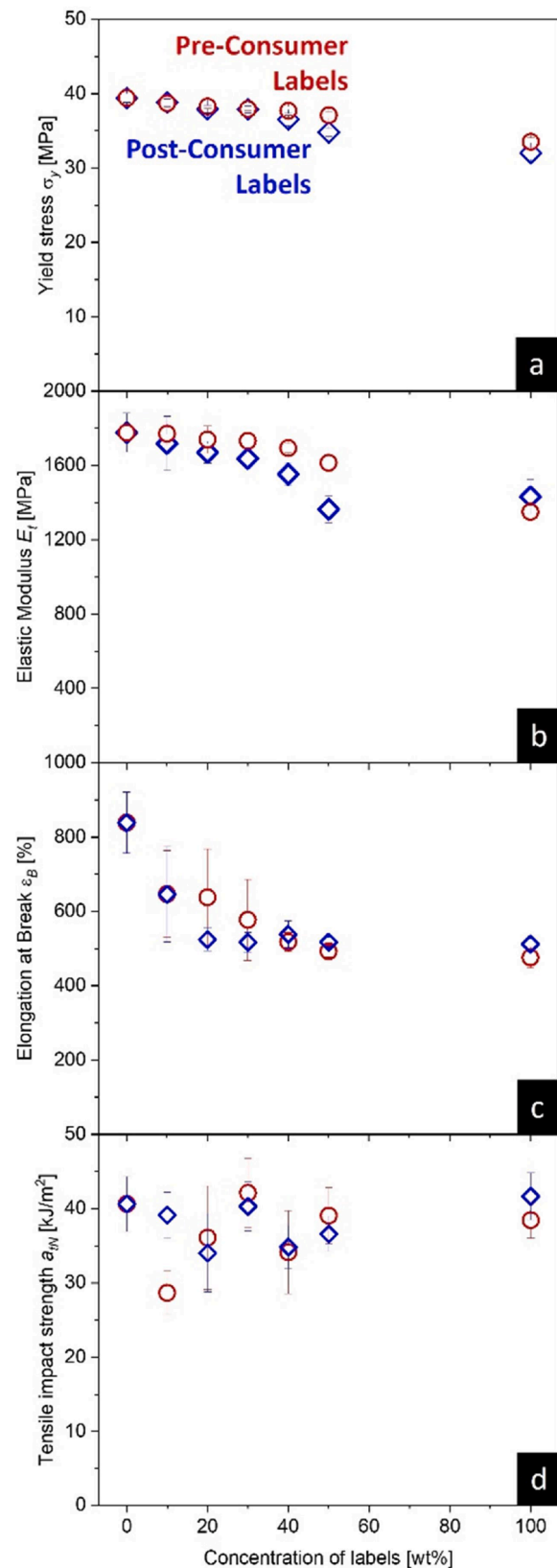


**Fig. 4.** (a) Yield stress ( $\sigma_y$ , MPa), (b) elastic modulus ( $E_t$ , MPa), (c) elongation at break ( $\epsilon_B$ , %) and (d) tensile impact strength ( $a_{IV}$ , kJ/m<sup>2</sup>) of blends containing pre- (red circles) and post-consumer (blue diamonds) labels. (For interpretation of the references to color in this figure legend, the reader is referred to the web version of this article.)

virgin material (Fig. 4b). However, the addition of post-consumer labels was associated with more rapid decreases in  $E_t$ , with a threshold value of approximately 50 wt.% labels already resulting in a minimum  $E_t$  identical to that associated with pure post-consumer labels.

$E_B$  was much more sensitive to label content, with a 23% decrease associated with the addition of only 10 wt.% pre- or post-consumer labels (Fig. 4c). A threshold value of 40 wt.% pre-consumer labels resulted in a minimum identical to that associated with pure-pre consumer labels. The same effect was witnessed in post-consumer labels, however, at a lower threshold value of 20 wt.%.  $a_{IN}$  was highly unpredictable in blends comprising labels and virgin material (Fig. 4d).

The poorer mechanical properties of recycled labels compared to virgin PP can likely be attributed to impurities and agglomerates of pigments (Eyerer et al., 2008). However, polymer contamination can also lead to deterioration of mechanical properties (Van Belle et al., 2020; Karaagac et al., 2021; 2021b). It should be noted that poor quality recyclates and inhomogeneous recycle compositions resulting in inconsistent mechanical properties lead to high economic risk for industry (Schyns et al., 2021).

### 3.4. Chemical and biological analysis of pre- and post-consumer labels

Chemical analysis of unprocessed and processed pre- and post-consumer labels identified linear and cyclic hydrocarbons, aromatic compounds, unidentified hydrocarbons, and other unknown substances. Overall, 71 substances could be assigned Cramer Classes while 95 substances were unable to be identified. Most of the identified substances (73%) were classified as Cramer Class I (nontoxic with a threshold of 1800  $\mu\text{g}/\text{person}/\text{day}$ , Table S1). However, a considerable portion (21%) of the remaining identified substances were Cramer Class III (highly toxic with a threshold of 90  $\mu\text{g}/\text{person}/\text{day}$ ), with a much smaller number (6%) of Cramer Class II substances present (moderately toxic with a threshold of 540  $\mu\text{g}/\text{person}/\text{day}$ ) (Table 1).

7,9-Di-tert-butyl-1-oxaspiro(4,5)deca-6,9-diene-2,8-dione and 2,6-ditert-butylcyclohexa-2,5-diene-1,4-dione (common name: 2,6-Di-tert-butyl-p-benzoquinone), which are degradation products of antioxidants typically used in polymer production (García Ibarra et al., 2019), were present in all labels (both unprocessed and processed pre-consumer and processed post-consumer labels). 2,2-Dimethoxy-1,2-diphenylethanone, 2,6-di-tert-butyl-4-hydroxy-4-methylcyclohexa-2,5-dien-1-one and ethyl 3-(3,5-ditert-butyl-4-hydroxyphenyl)propanoate were identified in both unprocessed and processed pre-consumer labels but not post-consumer labels. This was likely due to dilution of substances to levels below the detection limit in the more heterogeneous

post-consumer labels, compared to the more homogenous pre-consumer labels.

[(1R,2R)-2-phenylcyclobutyl]benzene and (3,5-diphenylcyclohexyl)benzene can be associated with the presence of styrene-based substances and were only present in processed pre-consumer labels. This indicated that the concentrations of these substances may increase as a result of temperature or mechanical processing effects. Notably, biological analysis also led to positive results in the miniaturized Ames test. Both test conditions TA98-S9 and TA100+S9 indicated the presence of DNA-reactive, mutagenic substances in processed and unprocessed material. These strains cover a range of mutagens: TA98 monitors frameshift mutations and TA100 point mutations, with and without metabolic activation through liver enzymes (which indicates that more than one substance group could be responsible for the positive result). That said, while mutagenic effects were noted, the responsible substance or substance group could not be identified through chemical analysis. The positive result does, however, indicate that the direct use of labels in recycling must be approached cautiously.

Notably, over half of the substances identified, many of which were Cramer Class III, were associated with processed post-consumer labels, suggesting that this post-consumer material was considerably more critical than pre-consumer material. This is likely the result of systematic changes, processing and aging effects or accumulation of contaminants over the course of the material's service life or in the waste stream. It could also simply be the result of the pre-consumer labels selected for this study being coincidentally considerably different (polymer, coating, pigments) from the post-consumer labels.

It should be noted that only label migrates were analyzed, which would likely never contact a product being packaged using virgin material due to the exterior location of the label on the packaging. These migrates could, however, be more problematic in recycled products where their dispersed nature results in a greater probability of them interacting with the packaged product.

## 4. Conclusion

Labels exhibit similar mechanical properties to most recyclates and can be suitable for extrusion or injection molding applications of PP with minimal esthetic and olfactory requirements, such as plant pots, storage boxes, or waste containers. However, the undesirability of labels as a recycling fraction is perhaps justifiable. Pigments contained in labels can cause shifts in FT-IR bands and act as nucleating agents for  $\beta$ -spherulites causing melting peaks that can be confused with copolymers or multi-layered structures. This can disrupt common characterization and

**Table 1**

Cramer Class II and III substances identified in unprocessed and processed pre-consumer material and processed post-consumer material.

Substance	CAS No.	Pre-consumer		Post-consumer (processed)	Cramer class
		Unprocessed	Processed		
7,9-Di-tert-butyl-1-oxaspiro(4,5)deca-6,9-diene-2,8-dione	82304-66-3	×	×	×	III
2,6-ditert-butylcyclohexa-2,5-diene-1,4-dione	719-22-2	×	×	×	II
2,2-dimethoxy-1,2-diphenylethanone	24650-42-8	×	×	-	III
2,6-di-tert-butyl-4-hydroxy-4-methylcyclohexa-2,5-dien-1-one	10396-80-2	×	×	-	III
Ethyl 3-(3,5-ditert-butyl-4-hydroxyphenyl)propanoate	36294-24-3	×	×	-	II
[(1R,2R)-2-phenylcyclobutyl]benzene	20071-09-4	-	×	-	III
(3,5-diphenylcyclohexyl)benzene	28336-57-4	-	×	-	III
2,6-di(propan-2-yl)naphthalene	24157-81-1	-	-	×	III
3,5-dichloroaniline	626-43-7	-	-	×	III
Diphenylmethanone	119-61-9	-	-	×	III
Heptadecanenitrile	5399-02-0	-	-	×	III
Hexadecanenitrile	629-79-8	-	-	×	III
(4-methylphenyl)-phenylmethanone	134-84-9	-	-	×	III
Phenyl-(4-phenylphenyl)methanone	2128-93-0	-	-	×	III
Nonanenitrile	2243-27-8	-	-	×	III
Pentadecanenitrile	18300-91-9	-	-	×	III
2,4-ditert-butyl-6-nitrophenol	20,039-94-5	-	-	×	III
3,5-di-tert-butyl-hydroxybenzaldehyde	1620-98-0	-	-	×	II
2,6-ditert-butylphenol	128-39-2	-	-	×	II

quality control techniques used in the recycling sector. More importantly, labels also exhibit highly unpredictable melting properties that lead to problems in processing using the industry standard melt mass-flow rate. Linear mixing rules consequently cannot be applied to blends of labels and virgin material, meaning that recyclers may be unable to predict processing parameters and be forced to test and modify mold and machine parameters on a batch-by-batch basis at considerable effort and cost. The elongation at break of these blends is also highly sensitive to label content, meaning that even low (10 wt.%) quantities of labels will compromise the mechanical properties of virgin-recyclate blends. Labels present additional processing challenges and safety concerns in the form of Cramer Class III toxic substances, most of which appear in processed post-consumer labels due to the heterogeneous nature of this material stream. Potential DNA-reactive, mutagenic effects were detected with *in vitro* bioassays both before and after processing.

Labels can certainly be recycled and could have useful applications; however, they are a minor (just ~2% of the total mass of a bottle packaging product) and likely not economically viable fraction that would require additional processing and infrastructure changes to process. This small fraction would otherwise be incinerated or could, in light of very high circularity ambitions, be included (as a minor component) in a co-fed stream for chemical recycling technologies, such as pyrolysis. Other more viable recycling fractions are abundantly available. It is also worth noting that concentrating undesirable components, such as pigments, into a single, small, and easily removable label, might even enhance recycling as contaminants are restricted to a single packaging component. The use of compounds in labels, adhesives and pigments is also differently regulated compared to food-contact packaging material, which lends additional support to assigning labels a sacrificial ‘transport vector’ out of recycling streams. Alternatively, if use as a recyclate is intended, design for recycling principles should be applied during label, adhesive and pigment design. Setting aside their possible use as recyclate, labels can play a systemic role and serve as recyclability enablers for the base packaging material. The important role of labels in ambitious recycling schemes is, however, likely of a different systemic nature: Educating customers on how best to sort and recycle their packaging, which would likely have a far greater impact on reducing contamination, improving recyclates and scope of application.

### CRedit authorship contribution statement

**Jessica Schlossnikl:** Conceptualization, Writing – original draft, Writing – review & editing, Investigation. **Elisabeth Pinter:** Writing – original draft, Writing – review & editing, Investigation. **Mitchell P. Jones:** Conceptualization, Writing – original draft, Writing – review & editing. **Thomas Koch:** Investigation, Writing – review & editing. **Vasiliki-Maria Archodoulaki:** Funding acquisition, Project administration, Supervision, Writing – review & editing.

### Declaration of Competing Interest

The authors declare that they have no known competing financial interests or personal relationships that could have appeared to influence the work reported in this paper.

### Data availability

Data will be made available on request.

### Acknowledgements

The authors acknowledge the assistance of Elisa Mayrhofer and Veronica Osorio (Austrian Research Institute for Chemistry and Technology) in toxicology analysis. This research was funded by the FFG –

Austrian Research Promotion Agency, as part of the project ‘Pack2the-Loop’ (#907682). We thank the TU Wien Bibliothek for financial support through its Open Access Funding Program.

### Supplementary materials

Supplementary data associated with this article can be found, in the online version, at [10.1016/j.resconrec.2023.107299](https://doi.org/10.1016/j.resconrec.2023.107299).

### References

- Achillas, D.S., 2022. Thermal analysis in polymer recycling. *Therm. Anal. Poly. Mater.* 485–508. <https://doi.org/10.1002/9783527828692.CH14>. Available at.
- Agbaje, O.B.A., et al., 2017. Architecture of crossed-lamellar bivalve shells: The southern giant clam (*Tridacna derasa*, Röding, 1798). *R. Soc. Open Sci.* 4 (9) <https://doi.org/10.1098/rsos.170622>. Available at:
- ECR Austria (2022) *Verpackungsstammdaten: eine Empfehlung der ECR Austria Arbeitsgruppe ‘Verpackungsstammdaten’*. Available at: <https://ecr-austria.at/2022/10/03/verpackungsstammdaten/> (Accessed: 4 July 2023).
- Bakker, E.J., Rem, P.C., Fraunholz, N., 2009. Upgrading mixed polyolefin waste with magnetic density separation. *Waste Manage. (Oxf.)* 29 (5), 1712–1717. <https://doi.org/10.1016/j.wasman.2008.11.006>. Available at.
- Baur, E., Harsch, G., Moneke, M., 2019. *Werkstoff-Führer Kunststoffe: Eigenschaften-Prüfungen-Kennwerte*, 11th edn. Carl Hanser Verlag, München.
- FH Campus Wien (2020) *Circular Packaging Design Guideline: Design Recommendations for Recyclable Packaging*. Wien. Available at: <https://digital.obvsg.at/obvfwacc/download/pdf/8086818?originalFilename=true> (Accessed: 26 July 2023).
- Chen, X. et al. (2022) ‘Enabling mechanical recycling of plastic bottles with shrink sleeves through near-infrared spectroscopy and machine learning algorithms’. Available at: <https://doi.org/10.1016/j.resconrec.2022.106719>.
- Chéroux Asensio, R., et al., 2009. Analytical characterization of polymers used in conservation and restoration by ATR-FTIR spectroscopy. *Anal. Bioanal. Chem.* 395, 2081–2096. <https://doi.org/10.1007/s00126-009-3201-2>. Available at.
- Christiani, J., Beckamp, S., et al., 2020. Was können die mechanische Aufbereitung von Kunststoffen und werkstoffliches Recycling leisten? In: Thiel, S., et al. (Eds.), *Energie aus Abfall*.
- Ciccola, A., et al., 2017. Azo-pigments effect on UV degradation of contemporary art pictorial film: A FTIR-NMR combination study. *Polym. Degrad. Stab.* 140, 74–83. <https://doi.org/10.1016/J.POLYMDEGRADSTAB.2017.04.004>. Available at:
- Clapp, J., 2012. The rising tide against plastic waste: Unpacking industry attempts to influence the debate. *Histories of the Dustheap: Waste, Material Cultures, Social Justice*, pp. 199–225.
- Cotrep (2022) *Bottles – PET and HDPE – general information on labels and sleeves - AG12*. Available at: <https://www.cotrep.fr/en/technical-study> (Accessed: 27 October 2023).
- Cozzarini, L., Marsich, L., Ferluga, A., 2023. Qualitative and quantitative contaminants assessment in recycled pellets from post-consumer plastic waste by means of spectroscopic and thermal characterization. *Poly. Eng. Sci.* 63 (4), 1126–1132. <https://doi.org/10.1002/PEN.26269>. Available at:
- da Silva, D.J., Wiebeck, H., 2020. Current options for characterizing, sorting, and recycling polymeric waste. *Prog. Rubber, Plast. Recycl. Technol.* 36 (4), 284–303. <https://doi.org/10.1177/1477760620918603>. Available at:
- Dealy John, M., Read Daniel, J., Larson Ronald, G., 2017. *Linear viscoelasticity—fundamentals. Structure and Rheology of Molten Polymers*, 2nd edn. Hanser Publishers, Munich, pp. 106–145.
- Eisenreich, N., Rohe, T., 2006. Infrared spectroscopy in analysis of plastics recycling. *Encycl. Anal. Chem.* <https://doi.org/10.1002/9780470027318.A2011> [Preprint]. Available at:
- Ersoy, O., Güler, D., Rençberoglu, M., 2021. Effects of grinding aids used in grinding calcium carbonate (CaCO<sub>3</sub>) filler on the properties of water-based interior paints. *Coatings* 2022 12 (1), 44. <https://doi.org/10.3390/COATINGS12010044>. Vol. 12, Page 44 Available at:
- EUNOMIA, 2022. PET Market in Europe: State of Play 2022. Available at: <https://www.eunomia.co.uk/reports-tools/pet-market-in-europe-state-of-play-2022/> (Accessed: 20 September 2023).
- European Commission (2022) ‘Proposal for a regulation of the European Parliament and of the Council on packaging and packaging waste, amending Regulation (EU) 2019/1020 and Directive (EU) 2019/904, and repealing Directive 94/62/EC’. Brussels. Available at: <https://eur-lex.europa.eu/legal-content/EN/TXT/?uri=CELEX:52022PC0677> (Accessed: 16 June 2023).
- Eyerer, P., Hirth, T., Elsner, P., 2008. *Polymer Engineering Technologien und Praxis, Polymer Engineering*. Springer, Berlin Heidelberg. <https://doi.org/10.1007/978-3-540-72419-3>. Available at:
- Gabriel, D.S. and Maulana, J. (2018) ‘Impact of plastic labelling, coloring and printing on material value conservation in the products of secondary recycling’. Available at: <https://doi.org/10.4028/www.scientific.net/KEM.773.384>.
- Gahleitner, M., Paulik, C., 2014. Polypropylene. *Ullmann’s Encyclopedia of Industrial Chemistry*. Wiley-VCH Verlag GmbH & Co. KGaA, Weinheim, Germany, pp. 1–44. [https://doi.org/10.1002/14356007.o21\\_o04.pub2](https://doi.org/10.1002/14356007.o21_o04.pub2). Available at:
- García Ibarra, V., et al., 2019. Non-target analysis of intentionally and non intentionally added substances from plastic packaging materials and their migration into food simulants. *Food Packag. Shelf Life* 21, 100325. <https://doi.org/10.1016/J.FPSL.2019.100325>. Available at:

- Grellmann, W., Seidler, S., 2011. *Kunststoffprüfung*. München, Hanser Verlag. <https://doi.org/10.3139/9783446429703>, 2. Auflage Available at:
- Grüner Punkt, 2023. 323 Mixed Polyolefin Items (MPO). Available at: <https://www.gruener-punkt.de/en/downloads> (Accessed: 27 October 2023).
- Guillén-Mallete, J., et al., 2021. Recycling printed polypropylene labels and polyolefins caps as chemical foaming agent to produce foam products. *J. Cell. Plast.* 57 (5), 733–756. <https://doi.org/10.1177/0021955X20959302>. Available at:
- Horodytska, O., Valdés, F.J., Fullana, A., 2018. Plastic flexible films waste management – A state of art review. *Waste Manage. (Oxf.)* 77, 413–425. <https://doi.org/10.1016/j.wasman.2018.04.023>. Available at:
- Juan, R., et al., 2021. Quantification of PP contamination in recycled PE by TREF analysis for improved the quality and circularity of plastics. *Polym. Test.* 100, 107273 <https://doi.org/10.1016/j.polymertesting.2021.107273>. Available at:
- Jung, M.R., et al., 2018. Validation of ATR FT-IR to identify polymers of plastic marine debris, including those ingested by marine organisms. *Mar. Pollut. Bull.* 127, 704–716. <https://doi.org/10.1016/j.marpolbul.2017.12.061>. Available at:
- Karaagac, E., et al., 2021a. Polypropylene contamination in post-consumer polyolefin waste: characterisation, consequences and compatibilisation. *Polymers* 13 (16), 2618. <https://doi.org/10.3390/polym13162618>. Available at:
- Karaagac, E., Koch, T., Archodoulaki, V.-M., 2021b. The effect of PP contamination in recycled high-density polyethylene (rPE-HD) from post-consumer bottle waste and their compatibilization with olefin block copolymer (OBC). *Waste Manage. (Oxf.)* 119, 285–294. <https://doi.org/10.1016/j.wasman.2020.10.011>. Available at:
- Klimchuk, M.R., Krasovec, S.A., 2012. Packaging desing. Successful Product Branding from Concept to Shelf. John Wiley & Sons, Inc., New Jersey [Preprint]. Available at: <https://www.wiley.com/en-us/Packaging+Design%3A+Successful+Product+Branding+From+Concept+to+Shelf%2C+2nd+Edition-p-9781118027066> (Accessed: 16 June 2023).
- Kühnel, T., et al., 2019. Influence of label impurities in recycling on the mechanical properties of PC/ABS materials. *Macromol. Symp.* 384 (1) <https://doi.org/10.1002/MASY.201900037>. Available at:
- Marchini, A., et al., 2021. Label information and consumer behaviour: evidence on drinking milk sector. *Agric. Food Econ.* 9 (1), 1–24. <https://doi.org/10.1186/S40100-021-00177-5/FIGURES/4>. Available at:
- Mauricio-Iglesias, M., et al., 2009. Application of FTIR and Raman microspectroscopy to the study of food/packaging interactions. *Food Addit. Contam.* 26 (11), 1515–1523. <https://doi.org/10.1080/02652030903148306>. Available at:
- Meyer, D., et al., 2023. Effect-detection by planar SOS-Umu-C genotoxicity bioassay and chemical identification of genotoxins in packaging migrates, proven by microtiter plate assays SOS-Umu-C and Ames-MPF. *Food Control* 147, 109546. <https://doi.org/10.1016/j.FOODCONT.2022.109546>. Available at:
- Munro, I.C., et al., 1996. Correlation of structural class with no-observed-effect levels: A proposal for establishing a threshold of concern. *Food Chem. Toxicol.* 34 (9), 829–867. [https://doi.org/10.1016/S0278-6915\(96\)00049-X](https://doi.org/10.1016/S0278-6915(96)00049-X). Available at:
- Nandiyanto, A.B.D., Oktiani, R., Ragadhita, R., 2019. How to read and interpret ftr spectroscopy of organic material. *Indones. J. Sci. Technol.* 4 (1), 97–118. <https://doi.org/10.17509/ijost.v4i1.15806>. Available at:
- Neubauer, C. et al. (2021) *Sortierung und Recycling von Kunststoffabfällen in Österreich: Status 2019*. Available at: [https://www.umweltbundesamt.at/studien-reports/publikationsdetail?pub\\_id=2357&cHash=55a375c9008e945f8c5b750745a179f6](https://www.umweltbundesamt.at/studien-reports/publikationsdetail?pub_id=2357&cHash=55a375c9008e945f8c5b750745a179f6) (Accessed: 2 October 2023).
- Plastics Europe (2022) *The Circular Economy for Plastics – A European Overview*.
- Rainer, B., et al., 2019. Mutagenicity assessment of food contact material migrates with the Ames MPF assay. *Food Addit. Contam.: Part A* 36 (9), 1419–1432. <https://doi.org/10.1080/19440049.2019.1634841>. Available at:
- Rundh, B., 2005. The multi-faceted dimension of packaging: marketing logistic or marketing tool? *Br. Food J.* 107 (9), 670–684. <https://doi.org/10.1108/00070700510615053>. Available at:
- Saikrishnan, S., et al., 2020. Thermo-mechanical degradation of polypropylene (PP) and low-density polyethylene (LDPE) blends exposed to simulated recycling. *Polym. Degrad. Stab.* 182 <https://doi.org/10.1016/J.POLYMEDEGRADSTAB.2020.109390>. Available at:
- Saunier, J., et al., 2017. Exploring complex transitions between polymorphs on a small scale by coupling AFM, FTIR and DSC: the case of Irganox 1076® antioxidant. *RSC Adv.* 7 (7), 3804–3818. <https://doi.org/10.1039/c6ra25632e>. Available at:
- Schröder, T., 2018. *Rheometrie-Viskosimetrie und Stoffdatenermittlung. Rheologie der Kunststoffe: Theorie und Praxis*, pp. 61–146.
- Schyns, G., Zoé, O., et al., 2021. Mechanical recycling of packaging plastics: A review. *Macromol. Rapid Commun.* 42 (3), 2000415 <https://doi.org/10.1002/MARC.202000415>. Available at:
- Sepperumal, U., Markandan, M., 2014. Growth of Actinomycetes and Pseudomonas sp., biofilms on abiotically pretreated polypropylene surface. *Eur. J. Zool. Res.* 3 (2), 6–17 [Preprint].
- Serranti, S., et al., 2015. An innovative recycling process to obtain pure polyethylene and polypropylene from household waste. *Waste Manage. (Oxf.)* 35, 12–20. <https://doi.org/10.1016/j.wasman.2014.10.017>. Available at:
- Siesler, H.W., et al., 2002. *Near-Infrared Spectroscopy*. Wiley-VCH.
- Singh Chouhan, H., et al., 2020. Investigating use of dimensional limestone slurry waste as fine aggregate in mortar. *Environ. Dev. Sustain.* 22, 2223–2245. <https://doi.org/10.1007/s10668-018-0286-9>. Available at:
- Sun, S., Ding, H., Hou, X., 2018. Preparation of CaCO<sub>3</sub>-TiO<sub>2</sub> Composite Particles and Their Pigment Properties. *Materials* 11 (7), 1131. <https://doi.org/10.3390/MA11071131>. 2018 Available at:
- Tavanai, H., et al., 2005. A study of the nucleation effect of pigment dyes on the microstructure of mass dyed bulked continuous filament polypropylene. *Iran. Polym. J.* 14 (3), 267–276.
- The International Organization for Standardization (2004) *Kunststoffe - Bestimmung der Schlagzähigkeit (ISO 8256:2004); Deutsche Fassung EN ISO 8256:2004*.
- The International Organization for Standardization (2012a) *Kunststoffe –Bestimmung der Schmelze-Massefließrate (MFR) und der Schmelze-Volumenfließrate (MVR) von Thermoplasten –Teil 1: Allgemeines Prüfverfahren (ISO 1133-1:2011); Deutsche Fassung EN ISO 1133-1:2011*.
- The International Organization for Standardization (2012b) *Kunststoffe –Bestimmung der Zugeigenschaften –Teil 2: Prüfbedingungen für Form- und Extrusionsmassen (ISO 527-2:2012); Deutsche Fassung EN ISO 527-2:2012*.
- The International Organization for Standardization (2020) *Kunststoffe –Polypropylen (PP)-Formmassen –Teil 2: Herstellung von Probekörpern und Bestimmung von Eigenschaften (ISO 19069-2:2016); Deutsche Fassung EN ISO 19069-2:2016*.
- Thoden van Velzen, E.U., et al., 2021. The impact of impurities on the mechanical properties of recycled polyethylene. *Packag. Technol. Sci.* 34 (4), 219–228. <https://doi.org/10.1002/PTS.2551>. Available at:
- Tom Learner, 2004. *Analysis of Modern Paints*. Getty Publications.
- Traxler, I., Kaineder, H., Fischer, J., 2023. Simultaneous modification of properties relevant to the processing and application of virgin and post-consumer polypropylene. *Polymers* 15 (7), 1717. <https://doi.org/10.3390/POLYM15071717/S1>. Available at:
- Van Belle, A.V., et al., 2020. Microstructural contributions of different polyolefins to the deformation mechanisms of their binary blends. *Polymers* 12 (5). <https://doi.org/10.3390/POLYM12051171>. Available at:
- von Vacano, B., et al., 2023. Elucidating pathways of polypropylene chain cleavage and stabilization for multiple loop mechanical recycling. *J. Polym. Sci.* 61 (16), 1849–1858. <https://doi.org/10.1002/pol.20230121>. Available at:
- White, A.R., 2012. Labels for packaging. *Packag. Technol.* 395–407. <https://doi.org/10.1533/9780857095701.2.395>. Available at:
- XENOMETRIX (2018) *Ames MPFTM 98/100 Microplate Format Mutagenicity Assay S. typhimurium TA98 and TA100, 2nd ed.* Available at: [https://www.xenometrix.ch/shop/mediafiles/Xeno%20Dateien/Short%20Protocol/Ames/Ames%20MPF%2098-100%20Short%20Protocol\\_2.0.pdf](https://www.xenometrix.ch/shop/mediafiles/Xeno%20Dateien/Short%20Protocol/Ames/Ames%20MPF%2098-100%20Short%20Protocol_2.0.pdf) (Accessed: 26 July 2023).
- Zheng, Q., Fan, J., 2022. Infrared spectroscopy method for detecting the content of antioxidant irganox 1076 in polypropylene. *MATEC Web. Conf.* 358, 01015. <https://doi.org/10.1051/mateconf/202235801015>. Available at:
- Zheng, Q., Fang, W., Fan, J., 2020. Determination of antioxidant irganox 1010 in polypropylene by infrared spectrometry polypropylene by infrared spectrometry. In: *IOP Conference Series: Earth and Environmental Science*. IOP Publishing Ltd. <https://doi.org/10.1088/1755-1315/514/5/052046>. Available at: